$e\Pi$: e-MERLIN Pulsar Interferometry project

Abstract

We propose an e-MERLIN Legacy Programme aimed at studying the physics of neutron star formation during supernovae and improving our understanding of Galactic structure. We will accomplish this with an astrometric program on radio pulsars with the goal of more than doubling the number of pulsars with accurate distances and velocities. Model independent velocities will place strong constraints on the mechanism responsible for the "kick" that is often imparted during the supernova in which the neutron star is formed and that makes the velocity of neutron stars the highest of any other class of stars. Such constraints are essential for probing the laws of physics at the extreme conditions that occur during supernova core-collapse. The astrometric observations will not only give the magnitude of the pulsar velocity, but also the direction that can be compared with the orientation of the spin-axis, pulsar wind nebulae and X-ray tori.

In many other aspects of the astrophysics and physics which can be probed with pulsars our understanding is enhanced by being able to derive accurate distances and velocities for them. Pulsars with known distance provide essential calibration points of the Galactic electron density structure models which in turn will improve distance estimates to pulsars without accurate astrometric data. Combined with observations of thermal radiation from the pulsar surface, distance measurements will constrain neutron star sizes with important implications for the neutron star equations of state. Knowing the proper motions also allows us to determine the birth locations of young pulsars and thus potentially associate them with the supernova remnants in which they were born and again allow us to study the physics of their birth. Moreover improved tests of theories of gravity and/or measuring the masses of neutron stars in binaries are also possible once we know the distance to a pulsar.

Team Members

Wouter Vlemmings	Argelander institute for Astronomy University of Bonn D-53121, Bonn, Germany Tel.: (+49) (0)228 733670	wouter@astro.uni-bonn.de
Ben Stappers	University of Manchester	Ben.Stappers@manchester.ac.uk
Michael Kramer		Michael.Kramer@manchester.ac.uk
Joseph Lazio	NRL	Joseph.Lazio@nrl.navy.mil
Shami Chatterjee	The University of Sydney	S.Chatterjee@physics.usyd.edu.au
Walter Brisken	NRAO	wbrisken@aoc.nrao.edu
Miller Goss		mgoss@nrao.edu
Bob Campbell	JIVE	campbell@jive.nl
Huib Jan van Langevelde	JIVE/Leiden Observatory	langevelde@jive.nl
Matthew Bailes	Swinburne University	mbailes@astro.swin.edu.au
Adam Deller		adeller@astro.swin.edu.au
Don Backer	UC Berkeley	dbacker@astro.berkeley.edu

Scientific Justification

Introduction

Neutron stars are one of the most extreme astrophysical objects known. They are formed in the supernova explosion which marks the end of massive star evolution and they have mass densities greater than that of atomic nuclei as well as the strongest magnetic fields ever measured. Their violent birth often imparts a "kick" which means that neutron stars have the highest space velocities of any other class of stars. Radio pulsars are rapidly rotating neutron stars which emit beams of radio emission from the magnetic poles. The large moment of inertia of the underlying neutron star means that as these radio beams sweep across the Earth and the received pulses provide a clock-like signal which has an accuracy rivalling the best atomic clocks on Earth. This remarkable property means that pulsars in binary systems can be used to perform some of the most stringent tests of the theories of gravity. These pulses also provide us with a probe of the interstellar medium via the frequency dependent delay generated by the free electrons along the line of sight.

In all aspects of the astrophysics and physics which can be probed with pulsars, the highest precisions are obtained if model-independent, accurate trigonometric distances and velocities are known. Because of its unique combination of resolution and sensitivity, e-MERLIN is excellent facility for increasing greatly the number of pulsars for which accurate parallaxes and the proper motion are measured.

Expanding the sample of pulsars for which we know their true space velocities provides us with vital insight into the physics of their formation in supernovae. Knowing the distance and the velocity also allows us to determine the birth locations of young pulsars and thus potentially associate them with the supernova remnants in which they were born and again allow us to study the physics of their birth. Accurate distances combined with our knowledge of the total electron content (obtained through the delay of the pulses) along the line of sight allow us to better determine the structure of the electron distribution in the Milky Way which has important implication for Galaxy modelling but also for predicting distances to pulsars without measured parallaxes. Moreover tests of theories of gravity and/or measuring the masses of neutron stars in binaries are also possible once we know the distance to a pulsar.

Pulsar astrometry

In astrometry, the basic observable is the position on the sky. When determining positions of individual objects, these measurements are necessarily relative in nature, and absolute positions are inferred when positions are determined relative to sources that define the International Celestial Reference Frame (ICRF; Ma et al. 1998). Over time, repeated position measurements allow a proper motion to be derived. The main consideration of such astrometric measurements is a long time baseline, limited by the stability of the reference frame and the variability of the frame-defining sources. When enough astrometric precision is possible, a trigonometric parallax may also be measurable. The primary consideration for such measurements is appropriate sampling over the Earth's orbital phase, not just a long time baseline.

Neutron stars emit over a broad range of wavelengths, and astrometric observations have been conducted at wavelengths from radio to X-rays. For example, Kaplan et al. (2007) have used optical observations with the Hubble Space Telescope to measure a proper motion $\mu = 107.8 \pm 1.2$ mas/yr and a parallax $\pi = 2.8 \pm 0.9$ mas for RX J0720.4-3125. At X-ray wavelengths, the resolution that can be achieved with the current generation of telescopes is a limiting factor, but Winkler & Petre (2007) have used the Chandra X-ray Observatory to measure a proper motion of 165 ± 25 mas/yr for the RX J0822-4300, in the center of the Puppis A supernova remnant.

The majority of known neutron stars are radio pulsars, and pulse timing is routinely used to refine their positions and proper motions. A subset of recycled ('millisecond') pulsars have rotation rates that are stable enough to permit sub-milliarcsecond astrometry based on pulse time of arrival. For example, van Straten et al. (2001) measure the general relativistic Shapiro delay for the binary pulsar J0437-4715, as well as a precise proper motion and parallax, based on pulse timing at Parkes. However, most pulsars do not have such stable rotation, particularly when they are young, and Very Long

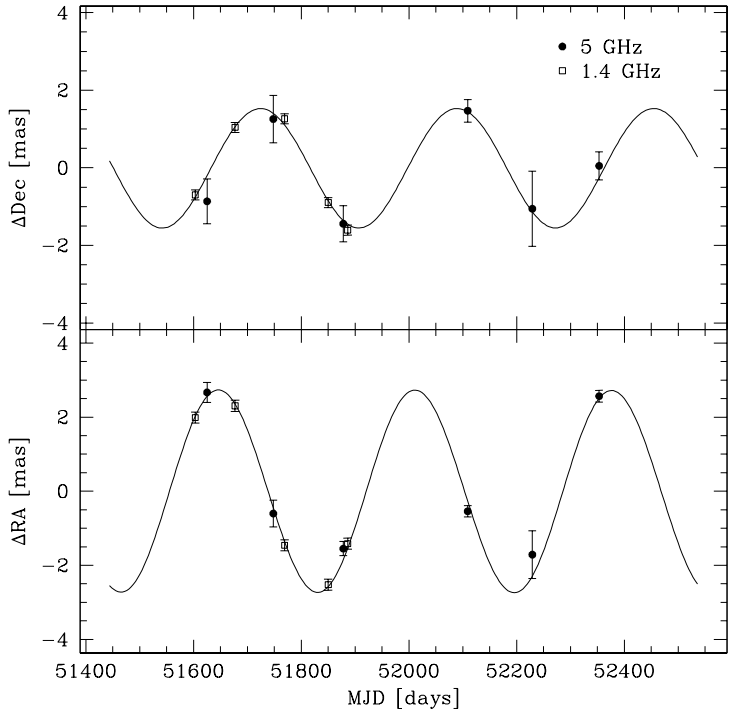

Figure 1: Parallax signature of PSR B1929+10 in right ascension and declination after subtracting the best-fit proper motion from the astrometric positions measured at 5 GHz (filled circles; Chatterjee et al. 2004) and 1.4 GHz (open squares; Brisken et al. 2002). Sinusoids corresponding to the best-fit parallax $\pi = 2.77$ mas are overplotted.

Baseline interferometry (VLBI) has usually been utilized to determine their astrometric parameters. Such efforts have a long history (e.g., Gwinn et al. 1986), but have become much more feasible with the Very Long Baseline Array (VLBA). (e.g., Fomalont et al. 1999; Brisken et al. 2000; Chatterjee et al. 2001; Brisken et al. 2002; Chatterjee et al. 2004, see Fig. 1) and recently with the Long Baseline Array (LBA; Deller et al. 2008a,b). Currently there are approximately 40 pulsars with astrometric parallaxes (Chatterjee et al., in prep.). *Its unique combination of sensitivity and resolution makes e-MERLIN the ideal instrument to make the next big step in pulsar astrometry, obtaining distances to pulsars out to* ~ 5 *kpc.*

Neutron star velocities

Parallaxes and proper motions lead to accurate model-independent transverse velocities for pulsars, which constrain the shape of the population velocity distribution. Additionally, parallaxes provide for improved electron density models, which in turn result in higher precision distance and velocity estimates for the entire pulsar population. Pulsar velocities also represent fossil information about the evolution of close binary systems and core collapse processes in supernovae. For high magnetic field objects, the entire range of velocities is of interest as supernova core collapse processes and interstellar accretion onto once-active but now dead pulsars are all constrained by model-independent velocity measurements. Currently, different analyses of the observations either claim an apparent bimodality of the NS velocity distribution (Arzoumanian et al. 2001, Cordes & Chernoff 1998), with a low (90 km/s) and high (500 km/s) velocity component, or a single component distribution at 400 km/s (Hobbs et al. 2005). To resolve this issue, and determine a pulsar velocity distribution that can then be reproduced by core collapse and acceleration models, at least double the number of pulsars with astrometric distances and velocities are needed. This will be achieved by the proposed e-MERLIN observations.

A number of physical mechanisms have been suggested to account for the high speeds, including

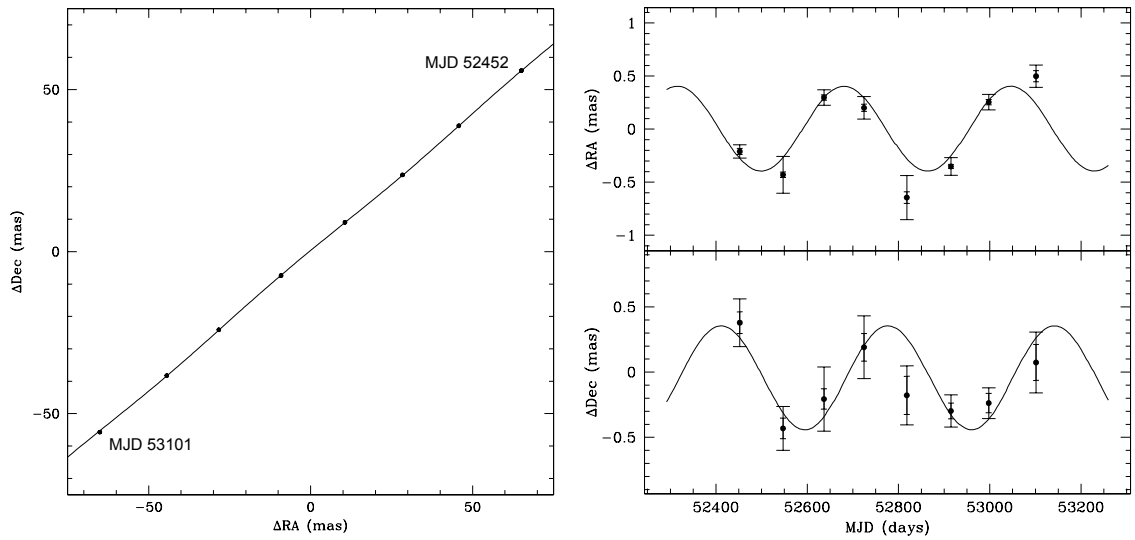

Figure 2: Left: The motion of PSR B1508+55 in right ascension and declination, with the best-fit proper motion and parallax model overplotted. The error estimates for each data point are smaller than the size of the points. Right: The parallax signature of PSR B1508+55 in right ascension and declination, after subtracting the best-fit proper motion from the astrometric positions. Curves corresponding to the best-fit parallax $\pi = 0.415$ mas are overplotted. The inner error bars indicate the random position uncertainties, while the outer error bars indicate the net uncertainties (random and systematic, added in quadrature). Both figures from Chatterjee et al. (2005).

the disruption of binaries through mass loss in supernovae (Blaauw 1961; Iben & Tutukov 1996) and the electromagnetic rocket effect (Harrison & Tademaru 1975), but it now appears likely that NS gain a large part of their observed velocity from a "birth kick" that involves asymmetries in the natal supernova explosion (Lai et al. 2001). The nature of the asymmetry remains unclear: while hydrodynamic or convective instabilities are plausible (Burrows & Hayes 1996; Janka & Mueller 1996), more exotic mechanisms such as asymmetric neutrino emission in the presence of strong magnetic fields cannot be ruled out (Arras & Lai 1999).

The high velocity tail of the pulsar birth velocity distribution is of particular interest, since these kicks impose the most stringent constraints on mechanisms for supernova core collapse. Currently, two-dimensional hydrodynamic models can provide a supernova detonation, a NS kick, and an asymmetric supernova remnant by invoking neutrino energy deposition (Scheck et al. 2004, 2006). However, the first full three-dimensional simulations of supernovae (Fryer 2004) have difficulty in producing the required magnitude of birth kicks, possibly implying the presence of extremely high magnetic fields $> 10^{15}$ G (Arras & Lai 1999) or some combination of the above effects (Socrates et al. 2005) in driving kicks.

Astrometric observations have established significant constraints on these questions. Specifically, a VLBA proper motion and parallax for PSR B1508+55 (Fig. 2, Chatterjee et al. 2005) provides a model independent transverse velocity estimate $V = 1083^{+103}_{-90}$ km/s , posing a significant challenge to those supernova core collapse simulations which do not provide large kicks. The extremely ordinary spin and spindown characteristics of the pulsar also challenge exotic kick scenarios that require extreme magnetic fields for high birth velocities.

For low magnetic field binary millisecond pulsars (MSPs), measured transverse velocities provide information on the degree of mass loss during the formation of the neutron star that also allowed a low-mass binary to remain bound. For solitary MSPs, velocity measurements may provide clues about any peculiarities in their formation process. Measurements also characterize the role of diffusion of stellar orbits in the Galaxy's gravitational potential, which is important for old stars.

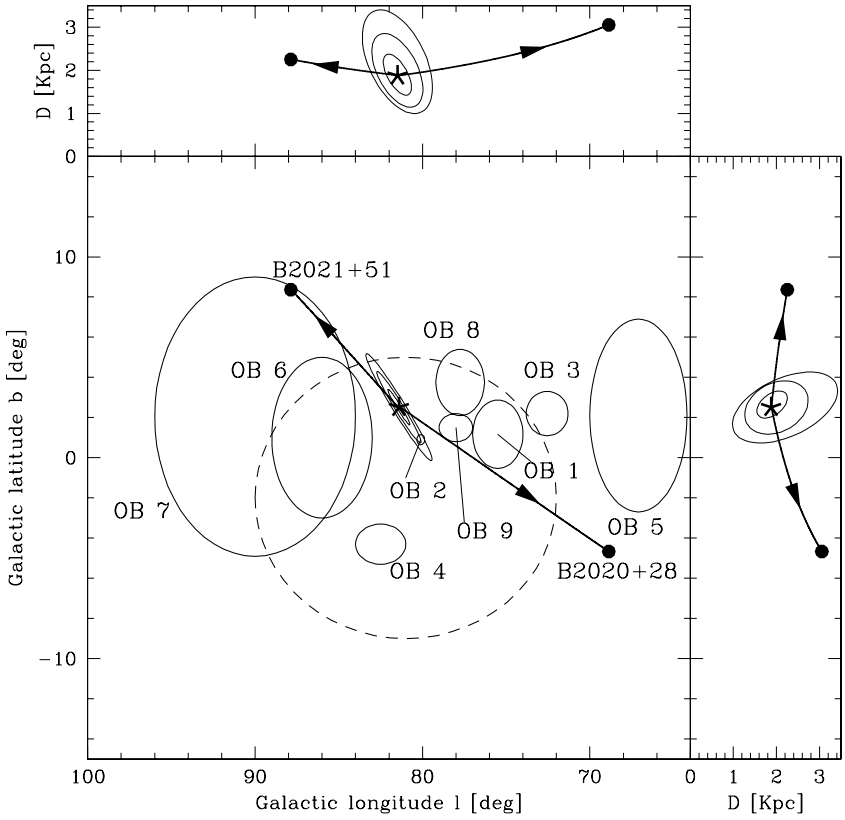

Figure 3: The 3-dimensional pulsar motion through the Galactic potential is shown for pulsars B2021+51 and B2020+28 (Vlemmings et al. 2004). The dashed circle represents the Cygnus superbubble, while the labeled solid ellipses are the Cygnus OB associations. The extent of OB 2 is unknown and only the center of the association is indicated. The thick solid lines indicate the pulsar paths, with the origin denoted by the starred symbol and the arrows pointing in the direction of motion. The current positions are indicated by the solid dots. The elliptical contours around the pulsars' origin in these panels indicate the 1, 2 and 3σ levels of the likelihood solution for the pulsar birth location based on the pulsar astrometric properties determined with the VLBA.

Other Science applications

As alluded to above, pulsar astrometry has a major impact on a number of other fields in astrophysics. Here we discuss a number of the astrophysical problems that will be addressed once e-MERLIN has provided a substantial increase of the number of pulsars with accurate parallaxes and/or proper motions.

-Galactic Electron Density models

Most pulsar distances are estimated from their dispersion measures (DM), using a model for the Galactic electron density such as Taylor & Cordes (1993, hereafter TC93) and Cordes & Lazio (2002, hereafter NE2001). In turn, because of its explicit incorporation of Galactic spiral structure, the TC93 model has been used as a surrogate for modeling the warm ionized medium, both in our Galaxy and others (e.g. Wood & Reynolds 1999, Roshi & Anantharamaiah 2000). Model-independent distances obtained from parallaxes provide essential calibration points for the electron density model. In particular, more parallaxes will allow much better modeling of the local interstellar medium (a weakness in the current model), thus providing better DM distances for nearby pulsars which are too weak to obtain parallaxes.

-Pulsar Birth Sites

Knowing the proper motion and distance to pulsars can help identify their birth sites, and clarify putative pulsar–SNR associations. True ages of both pulsars and their associated SNRs may also be estimated (or constrained) from the angular separation of the SNR and pulsar, and the pulsar proper motion (without the need for a parallax detection; see e.g. Zeiger et al. 2008). Similarly, accurate astrometry allows some pulsars to be traced back to their birth sites in stellar clusters (e.g. Hoogerwerf et al. 2001) or even to their companion star from which the pulsar was separated at birth (Fig.3; Vlemmings et al. 2004). This research area will become specifically important with the launch of GAIA in the near future. GAIA will provide astrometry for nearly all runaway OB stars and with a large number of pulsar proper motions and parallaxes we will be able to identify any possible runaway stars related to the pulsars and so determine kinematic ages. These put strong constraints on the pulsar birth properties. It is estimated that companion objects will be found for $\sim 10\%$ of the astrometrically observed pulsars.

-X-ray tori and the pulsar spin-axis

The direction and speed of motion of pulsars allows us to study the birth events of pulsars (i.e. the physics of core collapse supernovae). Using measurements of proper motions and polarisation properties of the pulse profiles, Johnston et al. (2005) were the first to show that the rotation and velocity vectors of young pulsars appear to be aligned. This configuration appears to be an imprint of the supernova explosion and is, for instance, possible if the birth period is small compared to the duration of a kick imparted to the newly born neutron star. Further information is obtained by combining astrometry data with high energy observations. Some pulsars (e.g. Crab and Vela) are observed to exhibit X-ray torii which appear also to be aligned with the rotation axis and hence are expected to be aligned with the velocity vector also (e.g. Ng & Romani, 2007). Together, combining astrometry data with radio polarision and X-ray data, it is possible to the increase the significance of this result and to search for age dependence as the motion in the Galactic potential is expected to alter this correlation.

-Interstellar Scintillation and Scattering

The characteristics of pulsar scintillation, i.e., scintillation time and bandwidth, depend in part upon the distribution of scattering material along the line of sight. Combining proper motion and parallax measurements with interstellar scintillation (ISS) observations of pulsars allows modeling of the distribution of scattering material, and thus contributes to modeling of the free electron density in the Galaxy. Identification of regions of enhanced scattering is particularly important, because they evidently signify locales where the interstellar medium has been stirred significantly by shocks. Chatterjee et al. (2001) demonstrate this analysis for PSR B0919+06, from which they find evidence for "clumps" with a probable scale size of 10 pc at the edges of the Local Bubble.

-Reference Frame Ties

Measuring the position of an object in two different coordinate frames permits the very fundamental operation of tying the two reference frames together. Since they are compact sources and are accessible to astrometry with different techniques and at different wavelengths, neutron stars are particularly well suited to such reference frame ties. Specifically, pulse timing provides radio pulsar positions in the Solar system reference frame, while VLBI measurements are tied to the distant quasars. Thus, simply measuring precise positions for recycled pulsars enables fundamental reference frame ties between the Solar system and the extragalactic ICRF (e.g. Bartel et al. 1996).

-Nuclear & High-Energy Astrophysics

Accurate distance measurements, in combination with observed thermal radiation from the neutron star surface, can be used to constrain the 'size' of the neutron star photosphere, with important implications for the NS Equation of State. For example, VLBA observations of PSR B0656+14

(Brisken et al. 2003) have been done to complement extensive X-ray/EUV/optical datasets with this aim.

A few or the pulsars in our sample are in binaries with white dwarfs which have been detected optically. Calculating an accurate distance to these sources will allow for remove a large amount of the uncertainty in comparing the observed optical parameters with those which are predicted by models for the cooling of white dwarfs (e.g. Bassa et al 2003).

Another subset of our sources are likely to be detected as gamma-ray pulsars by the recently launched GLAST satellite. Determining distances to these sources is of particular interest as it will allow us to determine what fraction of the pulsar spin down energy is converted into gamma-ray emission. We will be able to do this for the largest sample yet and thus will be an invaluable resource for those interested in modelling the pulsar emission process.

-Individual Objects & Tests of Theories of Gravity

For a number of pulsars, accurate astrometric measurements will provide important constraints on their origin. For example, the recently detected binary MSP J1903+0327 in the Galactic plane (Champion et al. 2008) is very massive and has an enigmatic eccentric orbit which is normally only observed for MSPs in globular clusters. Unless the pulsar was ejected at high velocity from a hitherto unknown nearby cluster, this discovery has important implications on MSP formation scenarios. A proper motion determination is needed to confidently rule out the possibility of ejection and will also significantly improve the mass determination, putting constraint on the pulsar equation of state. Additional interesting sources are PSR B1257+12, ith its planetary system, or which a distance is needed to constrain evolutionary models, and PSR J1012+5307 with its optical companion and consequently important role in connecting optical and radio reference frames.

Finally, our sample contains PSR B1534+12, which is one of just a handful of double neutron star binaries known and has been extensively used for tests of theories of gravity (e.g. Stairs et al 2002). However its usefulness for such tests is limited by the lack of a known distance to the source. This unknown distance means that the measured orbital period derivative is dominated by the error in the so-called Shklovskii term. Determining the distance, thought to be about 1 kpc, will provide another independent parameter for testing general relativity.

Serendipitous science: Pulsar Wind Nebulae

The relativistic wind, through which a pulsar loses most of its rotational energy, has largely unknown properties. However, when it is confined by the interstellar medium, it can create an observable pulsar wind nebula (PWN). Observations of PWN thus provide a unique opportunity to study the characteristics of the otherwise unknown relativistic wind. Only few PWN are known at radio wavelengths, mostly associated with young, energetic and/or fast pulsars (e.g. Gaensler et al. 2000). As the PWN will be faint, it will be masked by emission from the associated pulsar. This can be overcome by using pulsar gating/binning as has been demonstrated by a series of VLA and ATCA observations (Gaensler et al. 1998, Stappers et al. 2000). Our observations with e-MERLIN, will similarly be able to use binned data to search for weak emission around the pulsar, to a limit approximately an order of magnitude lower than with the ATCA/VLA observations. While the maximum detectable spatial resolution of e-MERLIN will not be optimal to detect the PWN that is often extended by over several arcminutes, our observations will still be able to put stringent constraints on PWN emission around our target sources.

Source Sample

Our initial sample is defined by pulsars at $\delta > -15^\circ$ for which no accurate parallax and proper motions are available. From these we select the pulsars that can be detected at sufficient SNR in 2 hours of total observation time at either C- or L-band to reach the limits set by the e-MERLIN astrometric stability (0.2/0.5 mas at C/L-band). Finally, we discard the pulsars with a dispersion measure distance > 7 kpc. Additionally we will include a number of slightly fainter pulsars for which a parallax or even only a proper motion determination will have enormous benefits, such as possibly

the double neutron star (PSR B1534+12) and the recently discovered eccentric binary pulsar (PSR J1903+0327; Champion et al. 2008). The sample that will be observed at C-band is given in Table 3 while the complete sample is given in Table 4.

We will observe the initial sample at L- and C-band to determine the calibrator situation, as we intend to use nearby in-beam calibrators to improve the astrometry. Due to its unmatched sensitivity, e-MERLIN will be able to detect in-beam calibrators for $\sim 30\%$ of our sources at C-band and for nearly all of the sources at L-band. From our initial sample of ~ 120 pulsars we will then select ~ 60 pulsars for astrometric observations, based on the calibrator situation.

Of the 60 pulsars that will be the target of our astrometric observations, it is expected that ≈ 40 significant parallaxes can be measured while proper motions or excellent upper limits will be determined for the majority of the sources. This will double the number of pulsars with accurate astrometry, which is essential when trying to define the pulsar velocity distribution. Additionally, the observations will provide an approximate 40 new line of sights to pulsars along which the Galactic electron density can be constrained. For comparison, for the current best NE2001 electron density model only 12 pulsars with parallax measurements were available.

e-MERLIN vs. VLBA

While the VLBA has been the instrument of choice for pulsar astrometry, the e-MERLIN upgrades will provide a number of advantages. The main advantage of e-MERLIN over the VLBA is its improved sensitivity. While e-MERLIN's lower resolution means that the sensitivity gain is negated for the pulsars themselves, the much better continuum sensitivity almost guarantees that in-beam calibrators can be found at L-band, whereas at the VLBA our experience showed that for only approximately 1 out of 3 pulsars a good calibrator could be found. As described below (and shown in Fig. 4), especially at L-band, in-beam calibrators are crucial to obtain good astrometric results. The requirement for in-beam calibrators at C-band is somewhat less, but even there, e-MERLIN will likely find suitable in-beam calibrators for $\sim 30\%$ of the pulsars. In addition to the sensitivity increase, e-MERLIN is also ideal for astrometry of pulsars in the Galactic plane, where scattering makes continent-scale VLBI ineffective.

Project timeline

While astrometric observations of the individual pulsars will take place over a period of 1–1.5 year, the total time for completion of the project is at between 3 and 3.5 years as not all astrometric observations will be feasible at the same time. The project can roughly be divided into 5 stages that are detailed in the attached flow-chart. After the initial snap-shot observations to determine the calibrator situation in Stage 0, the final target list and observing strategy will be decided in Stage 1. This will be approximately 6 months after the completion of the Stage 0 observations. The pulsar astrometric observations will commence in Stage 2 and will be spread over a total of 2.5 years. Each individual pulsar will, after 1 year of astrometric observations, move into Stage 3, which will consist of reduction following a pipeline that will be developed as part of the project. At the end of this stage, preliminary astrometric results will be obtained. In the final stage of the project the astrometry will be optimized by extensive error analysis based on our experience with previous VLBA and LBA observations and the legacy observations performed with e-MERLIN. We will for example be able to determine and remove systematic errors due to calibrator frequency dependent source structure by separately analysing the different data in different subbands.

Data products

Besides a catalog of pulsar positions, proper motions and parallaxes, the eΠ-project will, as a byproduct, also produce a number of other datasets and catalogs. Table.1 list these data products as well as the Stage in which they are produced. The intermediate data products will be released at a 'best effort' basis, meaning that the calibration will be optimized while the project progresses.

Table 1: Data products

Full sample	Snap shot images of calibrators and preliminary pulsar positions for strongest pulsars (no binning)	Stage 1
*e*Π-CCAT-0.5x	Astrometric Observations (epoch x) images of nodding and in-beam calibrators ($\approx$ 120 sources)	Stage 2
*e*Π-FV-0.5x	Images and uv-data of the entire field of view for each epoch	Stage 2
*e*Π-CCAT-1.0	Model images of nodding and in-beam calibrators	Stage 3
*e*Π-FV-1.0	Optimally reduced FOV data and full quality images	Stage 4
*e*Πcat-1.0	Pulsar astrometry catalog	Stage 4

References

Arras, P. & Lai, D. 1999, ApJ, 519, 745
Arzoumanian, Z., Chernoff, D. F., & Cordes, J. M. 2002, ApJ, 568, 289
Bartel, N., Chandler, J. F., Ratner, M. I., Shapiro, I. L., Pan, R., & Cappallo, R. J. 1996, AJ, 112, 1690
Bassa, C.G, van Kerkwijk, M.H. & Kulkarni, S.R. 2003, A&A, 403, 1067
Blaauw, A. 1961, Bull. Astron. Inst. Netherlands, 15, 265
Brisken, W. F., Benson, J. M., Beasley, A. J., Fomalont, E. B., Goss, W. M., & Thorsett, S. E. 2000, ApJ, 541, 959
Brisken, W. F., Benson, J. M., Goss, W. M., & Thorsett, S. E. 2002, ApJ, 571, 906
Brisken, W. F., Thorsett, S. E., Golden, A., & Goss, W. M. 2003, ApJ Lett., 593, L89
Burrows, A. & Hayes, J. 1996, Physical Review Letters, 76, 352
Champion, D. J., et al. 2008, Science, 320, 1309
Chatterjee, S., Cordes, J. M., Lazio, T. J. W., Goss, W. M., Fomalont, E. B., & Benson, J. M. 2001, ApJ, 550, 287
Chatterjee, S., Cordes, J. M., Vlemmings, W., Arzoumanian, Z., Goss, W. M., & Lazio, T. J. W. 2004, ApJ, 604, 339
Chatterjee, S., Vlemmings, W. H. T., Brisken, W. F., Lazio, T. J. W., Cordes, J. M., Goss, W. M., Thorsett, S. E., Fomalont, E. B., Lyne, A. G., & Kramer, M. 2005, ApJ Lett., 630, L61
Cordes, J. M., & Chernoff, D. F. 1998, ApJ, 505, 315
Cordes, J. M. & Lazio, T. J. W. 2002, ArXiv e-print, astro-ph/0207156
Deller, A. T., Tingay, S. J. & Brisken, W. 2008b, ArXiv e-print, astro-ph/0808.1598
Deller, A. T., Verbiest, J. P. W., Tingay, S. J. & Bailes, M. 2008a, ArXiv e-rint, astro-ph/0808.1594
Fomalont, E. B., Goss, W. M., Beasley, A. J., & Chatterjee, S. 1999, AJ, 117, 3025
Fryer, C. L. 2004, ApJ Lett., 601, L175
Gaensler, B. M., Stappers, B. W., Frail, D. A., & Johnston, S. 1998, ApJ Lett., 499, L69
Gaensler, B. M., Stappers, B. W., Frail, D. A., Moffett, D. A., Johnston, S., & Chatterjee, S. 2000, MNRAS, 318, 58
Gwinn, C. R., Taylor, J. H., Weisberg, J. M., & Rawley, L. A. 1986, AJ, 91, 338
Harrison, E. R. & Tademaru, E. 1975, ApJ, 201, 447
Hobbs, G., Lorimer, D. R., Lyne, A. G., & Kramer, M. 2005, MNRAS, 360, 974
Hoogerwerf, R., de Bruijne, J. H. J., & de Zeeuw, P. T. 2000, ApJ Lett., 544, L133
Iben, I. J. & Tutukov, A. V. 1996, ApJ, 456, 738
Janka, H.-T. & Mueller, E. 1996, A&A., 306, 167
Johnston, S., Hobbs, G., Vigeland, S., Kramer, M., Weisberg, J.M. & Lyne, A.G. 2005, MNRAS, 364, 1397
Kaplan, D. L., van Kerkwijk, M. H., & Anderson, J. 2007, ApJ, 660, 1428
Lai, D., Chernoff, D. F., & Cordes, J. M. 2001, ApJ, 549, 1111
Ma, C., Arias, E. F., Eubanks, T. M., Fey, A. L., Gontier, A.-M., Jacobs, C. S., Sovers, O. J., Archinal, B. A., & Charlot, P. 1998, AJ, 116, 516
Ng, C.-Y. & Romani, R.W. 2007, ApJ, 660, 1375
Roshi, D. A., & Anantharamaiah, K. R. 2000, ApJ, 535, 231
Scheck, L., Kifonidis, K., Janka, H.-T., & Müller, E. 2006, A&A., 457, 963
Scheck, L., Plewa, T., Janka, H.-T., Kifonidis, K., & Mller, E. 2004, Physical Review Letters, 92, 011103
Socrates, A., Blaes, O., Hungerford, A., & Fryer, C. L. 2005, ApJ, 632, 531
Stairs, I.H., Thorsett, S.E, Taylor, J.H. & Wolszczan, A. 2002, ApJ, 581, 501
Stappers, B. W., Gaensler, B. M., & Johnston, S. 1999, MNRAS, 308, 609
Taylor, J. H. & Cordes, J. M. 1993, ApJ, 411, 674
van Straten, W., Bailes, M., Britton, M., Kulkarni, S. R., Anderson, S. B., Manchester, R. N., & Sarkissian, J. 2001, Nature, 412, 158
Vlemmings, W. H. T., Cordes, J. M., & Chatterjee, S. 2004, ApJ, 610, 402
Winkler, P. F. & Petre, R. 2007, ApJ, 670, 635
Wood, K., & Reynolds, R. J. 1999, ApJ, 525, 799

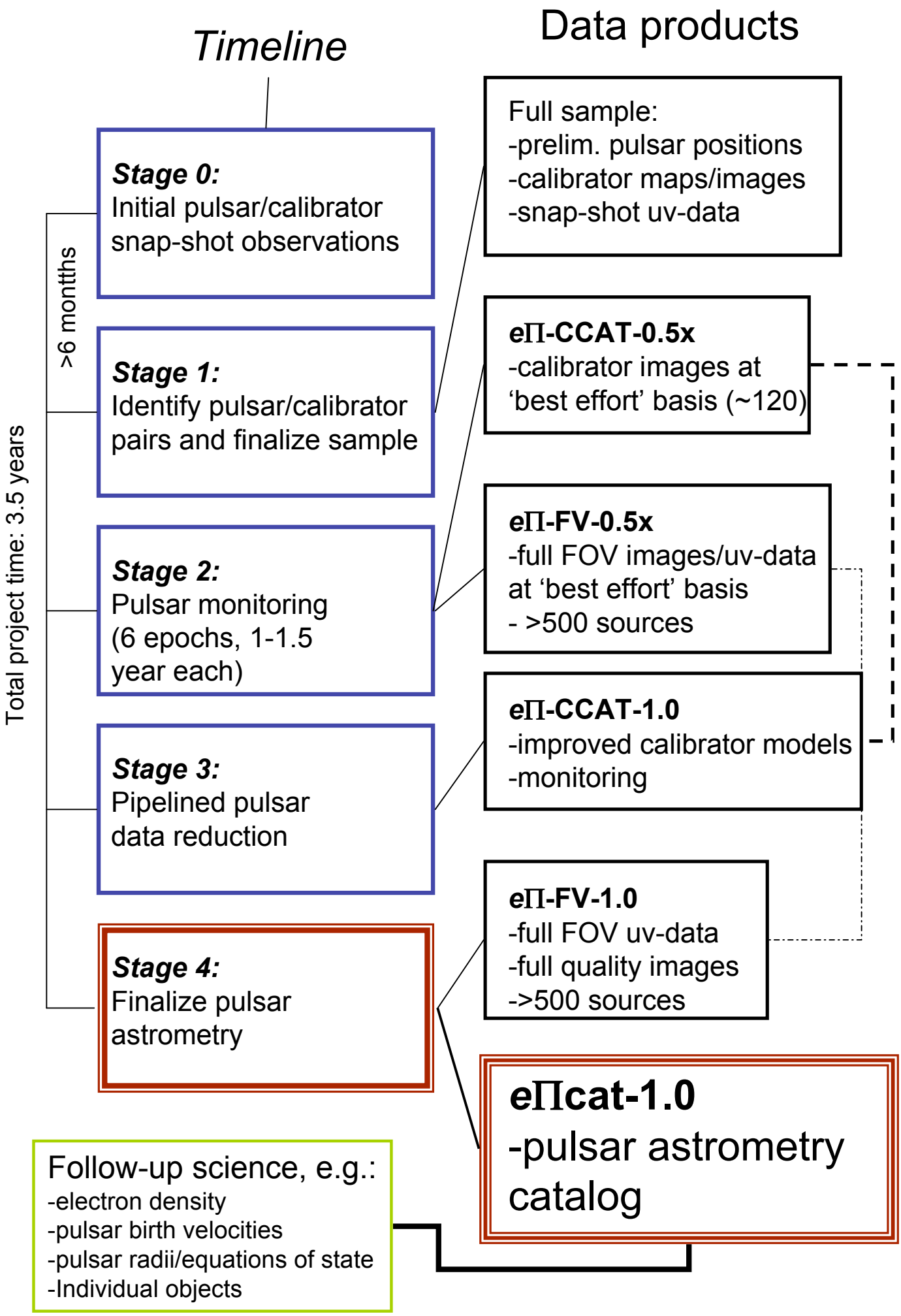
Timeline
Data products
Total project time: 3.5 years
>6 monthths
Stage 0:
Initial pulsar/calibrator snap-shot observations
Stage 1:
Identify pulsar/calibrator pairs and finalize sample
Stage 2:
Pulsar monitoring (6 epochs, 1-1.5 year each)
Stage 3:
Pipelined pulsar data reduction
Stage 4:
Finalize pulsar astrometry
Full sample:
-prelim. pulsar positions
-calibrator maps/images
-snap-shot uv-data
eΠ-CCAT-0.5x
-calibrator images at 'best effort' basis (~120)
eΠ-FV-0.5x
-full FOV images/uv-data at 'best effort' basis
- >500 sources
eΠ-CCAT-1.0
-improved calibrator models
-monitoring
eΠ-FV-1.0
-full FOV uv-data
-full quality images
->500 sources
eΠcat-1.0
-pulsar astrometry catalog
Follow-up science, e.g.:
-electron density
-pulsar birth velocities
-pulsar radii/equations of state
-Individual objects

Links to related data sets

Due to its unique nature, the astrometric monitoring observations have no direct link to existing data sets. However, as the unique e-MERLIN sensitivity will enable us to image a large number of weak radio sources in the field-of-view around the target pulsars and calibrators, the observations will also provide a data set of > 500 sources with fluxes $> 30/90\mu$Jy at C/L-band which will be of interest for creating for example an unbiased sample of extra-galactic radio galaxies. Additionally, a number of calibrator sources will effectively be monitored, allowing for a systematic study of their mas-scale structure evolution. The calibrator observations will be relevant for the "Astrometric survey of weak extragalactic sources with e-MERLIN" project (PI: Charlot). If possible with respect to the project timeline, we will also take into account planned observations by the "Astrometric survey" when deciding on potential calibrators for our astrometric pulsar monitoring.

Technical Justification

Total time request: 80 hr + 6 × 60 × 2 hr = 800 hr.

Sensitivity requirements

To reach the required astrometric accuracy with e-MERLIN, with its 40/150 mas resolution at C/L-band, a large SNR is required, as the positional accuracy will be limited by $\sigma_\theta \approx \theta_{FWHM}/\mathrm{SNR}$. To reach the $\approx$ 0.2/0.5 mas limit on C/L-band relative astrometry, the pulsar SNR needs to be $>$ 200/280. From previous VLBA observations we find that 6 epochs of observations with 0.5 mas positional accuracy allows for a parallax detection up to $\sim$ 5 kpc. The SNR on pulsar data can be increased by binning/gating the data. As described below the typical SNR improvement for the pulsars in our sample is a factor of 2–5. The observations will be taken in full continuum mode, 4 polarizations, 512 channels per subband, 16 subbands and 1 sec integration time. The L-band observations will use the full 400 MHz band between 1.3 and 1.7 GHz. If initial observations indicate that the RFI situation at L-band is such that 1024 channels offer a significant improvement during RFI excision, this can be accommodated by correlating only 2 polarizations. The C-band observations will use the 2 GHz bandwidth placed between 5 and 7 GHz. The regular observations do not require the Lovell telescope, though for individual pulsars we will investigate if its inclusion is worthwhile. With this setup, an rms (excluding Lovell) is reached of $\sim$ 15/45 μJy at C/L-band in 2 hours of observations (including overhead). Our target pulsars (Tables 3 & 4) are chosen to have a sufficient SNR when including gating/binning to reach our astrometric goals. Total observing time for the astrometric observations is thus 6 epochs × 2 hours × 60 sources = 720 hours.

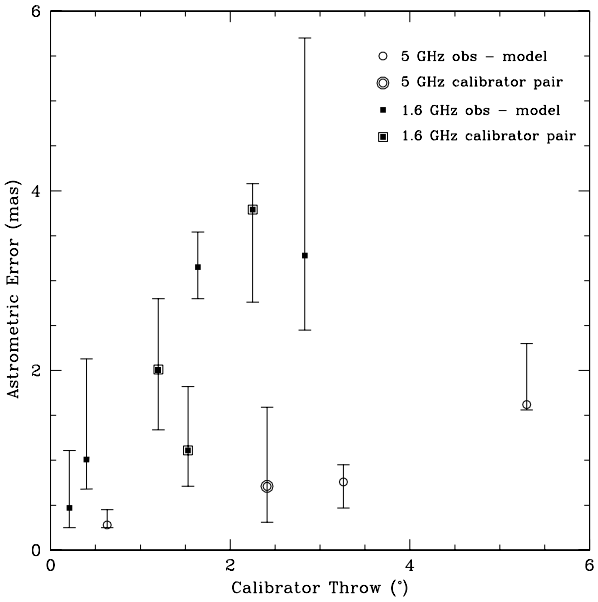

Figure 4: Astrometric position errors as a function of the angular separation between the target and the calibrator source. The 5 GHz data (open circles) are from astrometric observation of PSR B1929+10 and PSR B0355+54 (Chatterjee et al. 2005). The 1.6 GHz data (filled squares) include results from in-beam calibration for PSR B0919+06 (leftmost point; Chatterjee et al. 2001) and VLBI astrometry of circumstellar OH masers (Vlemmings et al. 2003).

In-beam calibration / primary beam gradients

As shown in Fig. 4, the astrometric accuracy that can be obtained by phase referencing is strongly dependent on the separation between the target and reference source. After initial calibration on a primary (nodding) phase reference source, residual calibration errors arise primarily from the unmodeled

ionosphere between target and reference source. Also seen in Fig. 4, the errors are significantly worse at L-band than at C-band. The remaining errors can be significantly reduced by using an secondary calibrator in the primary telescope beam, reducing the angular throw as well as the need for time extrapolation (e.g. Fomalont et al. 1999). Such a secondary in-beam calibrator can be much fainter than the primary calibrator. Due to the enormous continuum sensitivity of e-MERLIN, sources as weak as $\sim 300/900\mu$Jy can be used as in-beam calibrators at C/L-band. We thus expect to be able to detect suitable in-beam calibrators for $\sim 30\%$ of our sources at C-band and for all of the sources at L-band. At L-band, multiple in-beam sources will allow for the necessary modeling of atmospheric and instrumental phase gradients across the primary beam. At C-band the gradients will be significantly less, but will be modelled nonetheless using the extensive calibrator observations that will be available.

In an effort to identify the in-beam calibrators with sufficient flux, the project requires initial observations at C and L-band of our sources. At both bands, short, 10 min (on source) observations will be sufficient to detect all the potential calibrators. As we also want to examine the phase reference (nodding) calibrators, these preliminary observations thus require 60 hr at L-band and 20 hr at C-band, for a total of 80 hours including overhead. To maximize the field of view, the C-band observations will be taken using 2 polarization and 1024 channels across 16×128 MHz channels. Although this takes the effective FOV outside the half-power point of the typical telescope primary beam and will significantly reduce the sensitivity in the outer areas, it will allow us to detect possible in-beam calibrators so that the final pointing of the astrometric observations can be between the pulsar and the in-beam source. Although such wide FOV is not needed at L-band, the L-band observations will be also taken with 2 polarizations, 7-bit sampling and 1024 channels across the 16×32 MHz subbands, to enable better RFI excision.

Pulsar Gating & Pulsar Binning

Using pulsar gating the SNR of a pulsar can be increased by a significant fraction. By enabling the correlator to record data only when the pulsar is "on" the effective SNR increases depending on the pulsar duty cycle. The SNR increase can be expressed as $\sqrt(W_e/(P-W_e))$ where P is the pulse period and W_e the effective pulse width. The effective width is described by $W_e = \sqrt(W^2+\delta t^2+\delta t^2_{\rm scat}+\delta t^2_{\rm DM})$ and depends on the intrinsic pulse width W, the pulse broadening due to interstellar scattering $\delta t_{\rm scat}$ and due to dispersion across the frequency channel $\delta t_{\rm DM}$. It further depends on the maximum time resolution obtainable by the correlator δt, which for the e-MERLIN correlator is significantly less than any of the other contributions. The correlator will be able to use different gating parameters for each of the 32/128 MHz bands meaning that a C-band both $\delta t_{\rm DM}$ and $\delta t_{\rm scat}$ are negligible for the majority of the pulsars in our sample. At L-band $\delta t_{\rm DM}$ becomes comparable to the intrinsic pulse width for the pulsars with high dispersion measures while the scattering dominates for a handful of pulsars. For the pulsars in our sample we find that the increase in SNR as a result of the gating is of order a factor 2-5.

However, as in the pulsar gating only the signal is retained when the pulsar in "on", the SNR on any possible in-beam calibrators is significantly reduced. When using in-beam calibrators we will instead use pulsar binning. In this case, the pulsar cycle can be divided into up to 1000 bins. The "on"-pulse bins are then used for the pulsar, while the "off"-pulse bins are retained for detecting the in-beam calibrators. Ideally we will want to bin all the pulsar data in 64-1000 bins, and we will work closely with the e-MERLIN team towards implementing this binning in the e-MERLIN correlator. The gain in pulsar SNR is similar to the gating case described above with some added complexity in handling the processing of the binned pulsar data. The top quality ephemerides needed for pulsar gating/binning will be provided by the pulsar group at the Jodrell Bank Center for Astrophysics.

Requirements for pipeline processing/data archiving

The major requirement for the *e*Π-project will be the handling of the binned pulsar data. Members of our consortium, in particular a new PhD student in the JBCA pulsar group, will work closely with e-MERLIN staff to verify the system. The preliminary Stage 0 calibrator observations can be processed in the regular continuum pipeline. For the in-beam calibrator observations we will further develop pulsar astrometry scripting which exists within our consortium. This can be done supporting the standard pipeline developments. The data will be converted to UV-FITS files for processing in AIPS or EVLA data format for processing in CASA. The steps to reduce the in-beam calibration astrometric data are as follows:

1. Automated flagging and data editing based on observing logs, telescope data and other data assessment criteria.
2. $T_{\rm sys}$ based amplitude calibration.
3. Possible corrections at L-band using available ionospheric models.
4. On pulsar "off" binned data: Further amplitude, phase and bandpass calibration using calibrator models that will be refined when more epochs of observations become available.
5. On pulsar "off" binned data: Phase calibration and self-calibration using the nodding calibrators (with improving models).
6. On pulsar "off" binned data: Image and self-calibration on in-beam calibrators.
7. Use refined models describing phase slopes across the telescope beam to extrapolate calibration solutions. In the case of multiple in-beam sources, further interpolate the phase corrections between the sources.
8. Apply the combined corrections from the previous steps to the pulsar "on" binned data.
9. Image the pulsar and extract astrometric parameters.

While the regular 12 month data rights can be maintained for the continuum calibrator observations, the monitoring aspect of the proposal requires a deviation of the 12 month period for the pulsar data. The properly evaluate the astrometric data and produce the optimized results, we request at least 12 month period after the end of the monitoring period.

Management and Resource plan

In order to address the various aspects of the *e*Π-project observational strategy as well as those of the subsequent science, an international team has been assembled. A large number of the team members have extensive expertise in the planning of pulsar astrometry projects at the VLBA and LBA and the detailed analysis of resulting data.

The *e*Π-project will be coordinated by the principle investigator Wouter Vlemmings (University of Bonn, Germany) and the co-PI Ben Stappers (Jodrell Bank Center for Astrophysics, Manchester, U.K.). In the initial planning stages, the other team members will act as consultants. The final observational strategy will be decided upon by the coordinators after the observations that will determine the calibrator situation for each of the sources from the initial sample. Final source selection will also depend on these observations and will be decided by the entire project team. During the observations, the pulsar ephemerides necessary for the pulsar gating/binning will be provided by Michael Kramer (Jodrell Bank, U.K.), as all sources available to the Lovell telescope are regularly observed for timing observation by the pulsar group at the JBCA.

Once astrometric data is available, data reduction beyond the regular pipeline will proceed at a number of institutes. The institutes are listed in Table 2, which includes the estimated manpower resources that will be available as well as their responsibilities. Those members not in the table will contribute to the science appications and will act as regular consultants. These responsibilities include the different stages of data release as described above. The specific astrometric data reduction will be automated as much as possible. For previous VLBA experiments we have used AIPS scripting (by Walter Brisken, NRAO, USA) which we will adapt into ParselTongue scripting (developed as part of the EU funded ALBUS project; PI Huib Jan van Langevelde, JIVE, Netherlands). We will also investigate the application of ionospheric models developed at JIVE (Bob Campbell). The final check on data quality will be the responsibility of the team coordinators (Vlemmings & Stappers).

When legacy status is granted to the *e*Π-project, we expect to attract at least 2 PhD students to join the team. In Bonn, we will be part of the IMPRS (International Max-Planck Research School) for Astronomy and Astrophysics, which is a collaboration between the Max-Planck-Institut für Radioastronomie, the University of Bonn and the University of Cologne. Alternatively, a project legacy status will allow us to apply for funding through the Deutsche Forschungsgemeinschaft (DFG). A second PhD student will join the pulsar group at the JBCA and will work closely with the e-MERLIN team on commisioning the pulsar gating/binning.

Table 2: Project & Data reduction Resources & Responsibilities

Institute	Manager	Resources	Responsibilities
University of Bonn	Vlemmings	20%	Coordinator
	PhD student	100%	Data reduction / beam phase gradient corrections
University of Manchester	Stappers	10%	Coordinator
	Kramer		Pulsar Ephemerides
	PhD student	100%	reduction pipeline / data reduction
NRAO	Brisken	10%	consultant reduction pipeline / data reduction
JIVE	Campbell	5%	consultant ParselTongue scripting
			ionospheric modeling
University of Sydney	Chatterjee	10%	consultant data reduction

Legacy Justification

The e-MERLIN Legacy Programme is intended for large projects that provide large scientific impact while fully exploiting the enhanced capabilities provided by the e-MERLIN upgrade. Our proposed pulsar astrometry ($e\Pi$) programme fulfills these and several additional criteria to qualify for Legacy project status.

- The results that will arise from the $e\Pi$-project will be of *general and lasting importance to several different fields of astrophysics.* For instance, as described above, model independent distances are an important parameter in pulsar studies that aim to probe the laws of physics at extreme conditions, while combined with dispersion measures, they constrain the Galactic electron density.

- In addition to astrometric results for a large number of pulsars, the project will serendipitously provide a large database of multi-epoch observations of extra-galactic calibrator sources, which allows for monitoring of their mas-structure. These data sets will be provided to the community during the project soon after the observations have been taken.

- To reach its scientific goals, the $e\Pi$-project requires a large amount of dedicated time, both for the astrometric observations and for the initial observations to test the calibration situation and strategy. To reach the same scientific impact the number of smaller scale PATT proposals would be too large to be feasible, especially as the initial calibrator observations would decrease the effective efficiency of small individual proposals. While the total project duration is longer than the anticipated legacy project time of 5 semesters, this is a necessary consequence of the astrometric monitoring.

- Due to e-MERLIN unique sensitivity, the observations will detect several hundred radio sources in the field of view around the pulsar and calibrators, with even more sources to be found when the multi-epoch data sets are combined. Fully processed images as well as raw data sets will be made available compatible to VO standards. The total area covered by the observations to a 5σ level of $\sim 30/90\mu$Jy (C/L-band) will be > 20 square degrees for all observations combined.

Table 3: C-band target pulsars

Name	RA [h m s]	Dec [° ′ ″]	$S^{a}_{\mathrm{C-band}}$ mJy	DM Dist. [kpc]	binning gain (at C-band)
B0052+51	00:55:45.3	+51:17:24.9	0.63	2.40	4.7
B0136+57	01:39:19.7	+58:14:31.7	0.69	2.89	5.2
J0215+6218	02:15:56.6	+62:18:33.3	0.20	3.19	15.5
B0525+21	05:28:52.3	+22:00:01	1.01	2.28	4.1
B0540+23	05:43:09.6	+23:29:05	3.25	3.54	3.5
B0621-04	06:24:20.0	-04:24:50.4	1.12	4.28	3.7
B1642-03	16:45:02.0	-03:17:58.3	0.74	2.91	6.8
J1740+1000	17:40:25.9	+10:00:06.3	34.09	1.36	8.2
B1804-08	18:07:38.0	-08:47:43.2	5.42	3.60	3.4
B1820-11	18:23:40.3	-11:15:11	0.48	6.28	9.8
B1822-09	18:25:30.5	-09:35:22.1	2.42	1.00	4.2
B1828-11	18:30:47.5	-10:59:27.9	0.68	3.58	7.7
B1829-08	18:32:37.0	-08:27:03.6	0.66	4.75	5.0
B1830-08	18:33:40.3	-08:27:31.2	2.01	5.67	2.1
B1839+56	18:40:44.6	+56:40:55.4	0.52	1.70	5.3
B1838-04	18:41:05.6	-04:25:19.6	1.45	5.17	4.2
B1839-04	18:42:26.4	-03:59:59.8	1.37	4.15	2.1
B1845-01	18:48:23.5	-01:23:58.2	1.12	3.80	4.1
J1852-0635	18:52:57.3	-06:35:57	0.32	3.26	14.9
B1900+01	19:03:29.9	+01:35:38.3	0.54	4.40	5.5
B1903+07	19:05:53.6	+07:09:19.4	0.27	4.98	16.2
B1907+03	19:10:09.0	+03:58:28.0	0.54	2.95	5.5
B1944+17	19:46:53.0	+18:05:41.2	2.70	0.85	3.4
B1953+50	19:55:18.7	+50:59:55.2	0.45	1.80	6.2
B2022+50	20:23:41.9	+50:37:34.8	0.69	1.80	4.9
B2154+40	21:57:01.8	+40:17:45.8	1.92	5.58	3.5
B2255+58	22:57:57.7	+59:09:14.8	2.87	6.40	3.2
B2319+60	23:21:55.2	+60:24:30.7	2.80	3.21	3.7
B2324+60	23:26:58.6	+61:13:36.4	0.89	4.82	3.0
B2351+61	23:54:04.7	+61:55:46.7	1.01	3.31	4.9

[a] Extrapolated from L-band flux using spectral index (literature values where available, otherwise -2).

Table 4: All target pulsars

Name	RA [h m s]	Dec [° ′ ″]	S_{L-band} mJy	DM Dist. [kpc]	binning gain (at L-band)
B0011+47	00:14:17.7	+47:46:33.4	3.00	1.82	2.8
B0052+51	00:55:45.3	+51:17:24.9	1.50	2.40	4.7
B0059+65	01:02:32.9	+65:37:13.4	1.20	2.45	3.8
B0136+57	01:39:19.7	+58:14:31.7	4.60	2.89	4.6
B0138+59	01:41:39.9	+60:09:32.3	4.50	2.60	3.3
B0144+59	01:47:44.6	+59:22:03.2	2.10	1.91	4.1
B0148-06	01:51:22.7	-06:35:02.8	1.30	1.93	3.5
B0154+61	01:57:49.9	+62:12:25.9	1.90	1.61	4.3
J0215+6218	02:15:56.6	+62:18:33.3	3.70	3.19	8.0
B0301+19	03:04:33.1	+19:32:51.4	3.00	0.95	4.2
B0353+52	03:57:44.8	+52:36:57.7	1.90	4.73	2.5
B0402+61	04:06:30.0	+61:38:40.9	2.80	3.05	4.1
B0458+46	05:02:04.5	+46:54:06.0	2.50	1.78	4.0
B0525+21	05:28:52.3	+22:00:01	9.00	2.28	4.1
B0531+21	05:34:31.9	+22:00:52.0	14.00	2.00	1.9
B0540+23	05:43:09.6	+23:29:05	9.00	3.54	3.3
B0609+37	06:12:48.6	+37:21:37.3	4.00	1.49	3.9
B0611+22	06:14:17.1	+22:30:36	2.20	4.74	4.3
J0621+1002	06:21:22.1	+10:02:38.7	1.90	1.88	2.4
B0621-04	06:24:20.0	-04:24:50.4	2.00	4.28	3.7
B0626+24	06:29:05.7	+24:15:43.3	3.20	4.67	4.4
B0820+02	08:23:09.7	+01:59:12.4	1.50	1.44	4.9
B0834+06	08:37:05.6	+06:10:14.5	4.00	0.72	6.0
B0940+16	09:43:30.1	+16:31:37	1.40	1.76	3.1
J1012+5307[a]	10:12:33.4	+53:07:02.	3.00	0.52	1.0
B1112+50	11:15:38.4	+50:30:12.2	3.00	0.54	6.8
B1254-10	12:57:04.7	-10:27:05.8	1.20	2.22	4.6
B1257+12[a]	13:00:03.6	+12:40:56.5	2.00	0.62	1.8
J1518+4904	15:18:16.7	+49:04:34.2	4.00	0.70	3.9
B1534+12[a]	14:37:10.0	+11:55:55.6	0.60	0.68	5.6
B1540-06	15:43:30.1	-06:20:45.2	2.00	1.15	6.4
B1604-00	16:07:12.1	-00:32:40.8	5.00	0.59	4.7
J1643-1224	16:43:38.1	-12:24:58.7	4.80	4.86	1.0
B1642-03	16:45:02.0	-03:17:58.3	21.00	2.91	6.5
B1732-07	17:35:04.9	-07:24:52.4	1.70	4.32	4.4
B1737+13	17:40:07.3	+13:11:56.6	3.90	4.77	4.1
J1740+1000	17:40:25.9	+10:00:06.3	9.20	1.36	6.9
B1738-08	17:41:22.5	-08:40:31.8	1.40	3.50	4.1
B1745-12	17:48:17.4	-13:00:52.0	2.00	3.64	3.9
B1753+52	17:54:22.9	+52:01:12.3	1.60	3.56	4.2
B1804-12	18:06:06.7	-11:54:28.7	2.60	3.56	3.3
B1804-08	18:07:38.0	-08:47:43.2	15.00	3.60	2.9

Table 5: All targets –continued

Name	RA [h m s]	Dec [° ′ ″]	S_{L-band} mJy	DM Dist. [kpc]	binning gain (at L-band)
J1808-0813	18:08:09.4	-08:13:01.8	1.80	5.18	4.4
B1811+40	18:13:13.2	+40:13:39.0	1.10	4.32	5.6
B1818-04	18:20:52.6	-04:27:38.1	6.10	2.45	5.2
B1821+05	18:23:30.9	+05:50:24.3	1.70	3.01	4.0
B1820-11	18:23:40.3	-11:15:11	3.20	6.28	2.1
B1822-14	18:25:02.9	-14:46:52.6	2.60	5.45	2.2
B1822-09	18:25:30.5	-09:35:22.1	12.00	1.00	4.2
J1830-1135	18:30:01.7	-11:35:32	1.10	4.36	5.9
B1828-11	18:30:47.5	-10:59:27.9	1.40	3.58	4.7
J1831-1223	18:31:12.8	-12:23:31	1.20	5.51	4.6
B1829-08	18:32:37.0	-08:27:03.6	2.10	4.75	3.8
B1831-03	18:33:41.9	-03:39:04.3	2.80	5.07	4.4
B1831-04	18:34:25.6	-04:26:15.8	5.00	2.30	1.4
J1835-1106	18:35:18.2	-11:06:15.1	2.20	3.08	3.0
J1835-1020	18:35:57.5	-10:20:04.8	1.90	2.57	4.4
B1834-04	18:36:51.7	-04:36:37.6	1.80	4.62	3.3
B1834-10	18:36:53.9	-10:08:08.3	3.70	5.39	3.7
B1834-06	18:37:14.6	-06:53:02.1	2.50	4.93	3.2
J1840-0815	18:40:13.7	-08:15:10.6	1.40	4.43	5.0
J1840-0809	18:40:33.3	-08:09:03.3	2.30	5.81	4.1
B1839+56	18:40:44.6	+56:40:55.4	4.00	1.70	5.3
B1838-04	18:41:05.6	-04:25:19.6	2.60	5.17	2.0
B1839+09	18:41:55.9	+09:12:07.3	1.70	2.49	5.0
B1839-04	18:42:26.4	-03:59:59.8	4.40	4.15	2.1
J1843-0459	18:43:27.6	-04:59:30.4	1.70	6.15	2.6
J1843-0000	18:43:27.9	-00:00:40.9	2.90	2.83	4.5
B1841-05	18:44:05.1	-05:38:34.1	2.20	6.18	1.9
J1844+00	18:44:11	+00:35	8.60	6.65	2.6
B1841-04	18:44:33.4	-04:33:12.4	1.10	2.78	5.6
B1842+14	18:44:54.8	+14:54:14.1	1.50	2.23	4.8
B1842-04	18:45:34.7	-04:34:29.8	1.60	4.61	3.5
J1845-0743	18:45:57.1	-07:43:38.4	2.70	5.85	1.5
B1844-04	18:47:22.8	-04:02:14.1	4.30	3.12	4.1
B1845-01	18:48:23.5	-01:23:58.2	8.60	3.80	3.9
B1846-06	18:49:06.4	-06:37:06.9	1.40	3.68	4.6
J1852-0635	18:52:57.3	-06:35:57	5.90	3.26	5.4
J1901+0413	19:01:10.3	+04:13:51	1.10	6.91	8.1
J1901-0906	19:01:53.0	-09:06:10.8	3.10	2.42	5.0

Table 6: All targets –continued

Name	RA [h m s]	Dec [° ′ ″]	S_{L-band} mJy	DM Dist. [kpc]	binning gain (at L-band)
B1900+05	19:02:42.6	+05:56:25.9	1.20	3.91	4.6
B1900+01	19:03:29.9	+01:35:38.3	5.50	4.40	4.5
J1903+0327[a]	19:03:05.7	+03:27:19.2	1.30	6.45	2.0
J1904+0004	19:04:12.7	+00:04:05.3	2.10	6.43	1.8
B1903+07	19:05:53.6	+07:09:19.4	1.80	4.98	4.9
B1905+39	19:07:34.6	+40:02:05.7	1.80	1.76	4.0
B1907+10	19:09:48.6	+11:02:03.3	1.90	4.31	3.7
B1907+03	19:10:09.0	+03:58:28.0	1.50	2.95	5.5
B1911+13	19:13:24.3	+14:00:52.7	1.20	5.07	4.3
B1911-04	19:13:54.1	-04:40:47.6	4.40	3.22	6.8
B1913+10	19:15:29.9	+10:09:43.7	1.30	5.32	3.6
B1914+13	19:16:58.6	+13:12:50.0	1.20	6.16	3.1
B1915+13	19:17:39.7	+13:53:56.9	1.90	4.07	3.7
B1919+21	19:21:44.8	+21:53:02.2	6.00	0.66	5.6
B1935+25	19:37:01.2	+25:44:13.6	2.30	2.76	2.9
B1944+17	19:46:53.0	+18:05:41.2	10.00	0.85	3.4
B1952+29	19:54:22.5	+29:23:17.2	8.00	0.42	4.8
B1953+50	19:55:18.7	+50:59:55.2	4.00	1.80	6.1
B2000+32	20:02:04.4	+32:17:18.3	1.20	6.68	3.9
B2003-08	20:06:16.3	-08:07:01.9	2.80	2.01	2.2
B2022+50	20:23:41.9	+50:37:34.8	2.20	1.80	4.8
B2043-04	20:46:00.1	-04:21:26.0	1.70	3.83	6.6
B2044+15	20:46:39.3	+15:40:33.6	1.70	2.56	4.7
B2106+44	21:08:20.4	+44:41:48.8	5.40	5.28	1.7
B2110+27	21:13:04.3	+27:54:02.2	1.10	1.39	7.0
B2111+46	21:13:24.3	+46:44:08.7	19.00	4.99	2.4
B2148+52	21:50:37.7	+52:47:49.6	2.00	5.67	3.2
B2154+40	21:57:01.8	+40:17:45.8	17.00	5.58	3.5
B2217+47	22:19:48.1	+47:54:53.9	3.00	2.45	6.1
B2224+65	22:25:52.4	+65:35:34.0	2.00	2.00	4.4
B2255+58	22:57:57.7	+59:09:14.8	9.20	6.40	3.1
B2303+30	23:05:58.3	+31:00:01.7	2.20	3.92	6.7
B2306+55	23:08:13.8	+55:47:36.0	1.90	2.42	3.6
J2317+1439	23:17:09.2	+14:39:31.2	4.00	1.89	1.0
B2319+60	23:21:55.2	+60:24:30.7	12.00	3.21	3.7
B2324+60	23:26:58.6	+61:13:36.4	4.40	4.82	2.8
B2334+61	23:37:05.7	+61:51:01.6	1.40	2.47	3.6
J2346-0609	23:46:50.4	-06:09:59.5	2.00	1.96	3.9
B2351+61	23:54:04.7	+61:55:46.7	5.00	3.31	4.9

[a] added for specific science reasons